## Supporting Information

# Homoleptic Copper(I) Phenylselenolate Polymer as A Single Source Precursor for Cu₂Se Nanocrystals. Structure, Photoluminescence and Application in Field-Effect Transistor

Kam-Hung Low,[a] Cheng-Hui Li,[b] Vellaisamy A. L. Roy,[c] Stephen Sin-Yin Chui,[a] Sharon Lai-Fung Chan[a] and Chi-Ming Che*[a,b]

[a] Institute of Molecular Functional Materials, Department of Chemistry and HKU-CAS Joint Laboratory on New Materials, The University of Hong Kong, Pokfulam Road, Hong Kong SAR. Fax: 852 2857 1586; Tel: 852 2859 2154; E-mail: cmche@hku.hk
[b] Coordination Chemistry Institute and the State Key Laboratory of Coordination Chemistry, School of Chemistry and Chemical Engineering, Nanjing University, Nanjing 210093, People's Republic of China.
[c] Department of Physics and Materials Science, City University of Hong Kong, Tat Chee Avenue, Kowloon, Hong Kong SAR

**Instrumentation.** Scanning electron microscopic (SEM) image was recorded by the LEO 1530 scanning electron microscope. Transmission electron microscopic (TEM) image, energy dispersive X-ray spectroscopy (EDS) and selected area electron diffraction (SAED) pattern were recorded by FEI Philips Tecnai 20 transmission electron microscope. Thermogravimetric data were obtained using a Perkin-Elmer Thermal Analyzer TGA-7 under a stream of flowing $N_2$. Elemental analyses of solid samples were performed at the Institute of Chemistry, Chinese Academy of Sciences. ^{1}H-NMR spectra of solid samples dissolved in $d$-CHCl$_3$ were recorded with Bruker DPX 300 FT-NMR spectrometer with chemical shift (in ppm) relative to tetramethylsilane. The organic vapor evolved during thermolysis of $[Cu(SePh)]_\infty$ solid was condensed on a cold-finger and dissolved in diethyl ether to give a light yellow ethereal solution, which was analyzed by GC-MSD (Agilent 6890N and 5973N) equipped with HP-5 column. Steady-state emission spectra at 298K and 77K were recorded on SPEX Fluorolog-II Model F111 spectrophotometer. Inductively coupled plasma mass spectra (ICP-MS) were measured with a Agilent 7500a ICP-MS.

**Structure Determination using Powder X-ray Diffraction.** *a) Sample preparation and data collection:* The freshly prepared solid sample of $[Cu(SePh)]_\infty$ was ground into a fine powder and was loaded onto a glass holder or a sealed glass capillary. Replicate X-ray diffraction datasets were collected in a Bragg-Brentano or capillary transmission geometry by Bruker D8 ADVANCE X-ray diffractometer with CuKα radiation (λ = 1.5418 Å, rated as 1.6 kW). Data collection parameters were the following: 2θ range = 3–60º, step size = 0.02° in 2θ, speed of scan = 10 second/step. The phase-purity of solid samples of

[Cu(SePh)]$_\infty$ **1** and [Cu(SeMe)]$_\infty$ **2** were checked by ICDD (International Center fro Diffraction Data, PDF-2 Release 2004) database match search and the sample in each case examined was found to be free of crystalline $Cu_2O$ impurity.

*b) Structure solution:* Using Indexing program DICVOL04[1] and TREOR,[2] calculation based on the first 14 diffraction maxima from the diffractograph of [Cu(SePh)]$_\infty$ gave a reduced tetragonal lattice [$a' = b' = 12.150(2)$ Å, $c = 4.176(3)$ Å, $V = 1222.8.8$ Å$^3$, $M(14) = 23.3$, $F(14) = 27.7$ (0.0095,56)] or monoclinic unit cell: [$a = 12.1812(2)$ Å, $b = 12.1329(3)$ Å, $c = 3.9772(3)$ Å, $\beta = 94.384°$, $V = 586.08$ Å$^3$, $M(14) = 84.5$, $F(14) = 93.0$ (0.0036,42)]. The tetragonal unit cell was assigned due to (i) the priority of high symmetry lattice with *ca.* 2 times larger cell volume of the latter one, (ii) a characteristic ratio of the first four diffraction maxima in a order of q:$\sqrt{2}$q:2q:$\sqrt{5}$q, where q = 1/d. The true cell length *a* axis of the tetragonal lattice can be derived by a geometric transformation [$a = a'\sqrt{2}$] and the first four diffraction maxima were indexed as [110], [200], [220] and [310] reflections. Initial lattice parameters were refined by Pawley fit algorithm.[3] Background, zero-point, and profile shape parameters were refined together to achieve the improved profile fitting (reliability indicator $\chi < 2$–5). Followed space group assignment was performed by a probability (trial and error) approach in which the systematic absences of the extracted intensities were evaluated by CHECKCELL (available at http://www.ccp14.ac.uk/tutorial/lmgp/index.html#checkcell). Space group *P*4$_2$/*n* (number 86) was chosen for [Cu(SePh)]$_\infty$ because (i) all observable diffraction peaks in its diffractogram were indexed and matched with the calculated Bragg peak positions, (ii) high occurrence (275 times for *P*4$_2$/*n*, 213 times for *P*4/*n*, 85 times for *P*4/*ncc*, 79 times for *P*4/*nmm*) among the common centrosymmetric space groups appeared in Cambridge Structural Database (CSD 2005 release). According to its unit cell volume, eight formula mass units of [Cu(SePh)]$_\infty$ were used per each asymmetric unit. Initial model for structure solution was built and written as a MOL file format by the program ISIS DRAW version 2.14, which was later converted to sets of fractional coordinates written in a Z-MARTIX file format by program Babel (http://www.eyeopen.com/babel/) or OPENBABEL (http://openbabel.sourceforge.net). Bond distances restraints (Å) were: C($sp^2$/$sp^3$)-H 0.96, C($sp^2$)-C($sp^2$) 1.39, C($sp^2$)-Se 1.95, and Cu-Se 2.35 Å. Bond angle

restraints (º) for $C(sp^2)$-$C(sp^2)$-$C(sp^2)$ and $C(sp^2)$-$C(sp^2)$-Se were 120 and 109.5 respectively. The positions of carbon and hydrogen atoms of the phenyl rings were constrained into the same plane.

Structure solution calculations were initiated by a global optimization of experimental diffraction pattern using simulated annealing implemented in the program DASH[4]. A large number of trial structures (~10,000) were calculated using default parameters/setting. No preferred orientation correction was applied. A total of six positional parameters (XYZ) for the CuSePh fragment, and four orientation angles of the Se-ligand were varied. The ∠Cu–Se–C was fixed at around 109º and the torsion angle ∠Cu–Se–C–C was allowed to be freely varied. When the calculated $\chi^2$ was reduced to a minimal level (*ca.* within 5 times of the original profile $\chi^2$ value), the structure was solved. Selected structure solutions were examined and judged based on chemical and physical knowledge as well as the graphical fit between the calculated and experimental diffractographs.

*c) Structure refinement:* Prior to any structural refinement, the chemically sensible structure solution was manually adjusted so as to remove those unrealistic close non-bonded contacts by applying the appropriate sets of atom-atom distance restraints (minimum non-bonded distances of 2.0 Å and 2.5 Å for H···H and H···C respectively). For instance, when those bad contacts disappeared, the corresponding weighing factors of those distance restraints were reduced accordingly or the restraints were removed. The model adjustment process was repeated many times until there were no overlapped atoms or unrealistic bad contacts for non-bonded atoms. Subsequent Rietveld profile refinement by the full matrix least squares was carried out by GSAS/EXPGUI suite programs.[5] Scattering factors, corrected for real and imaginary anomalous dispersion terms were taken from the internal library of GSAS. Overall scale factor and the coefficients of the linear interpolation background function were refined. Profile shape parameters (Pseudo-Voigt function),[6] instrumental parameters (S/L) and (H/L), sample displacement (shft), Gaussian peak width (GW) and the Lorentzian peak broadening factor due to the microstrain effect of crystallites (LY) were sequentially refined. When the refinement of all these non-structural parameters became converged with a negligible (shift/esd)$^2$ value, the model-biased profile refinement was switched in which the unit cell parameters (*a, b, c* and *β*), atomic coordinates, background, peak profile parameters

were refined together to give the final $R_p$, $R_{wp}$, $R_{exp}$ and $R_F$ factors. Crystallographic data (excluding structure factors) for [Cu(SePh)]$_\infty$ **1** has been deposited in the Cambridge Crystallographic Data Center (CCDC) as supplementary publication numbers: CCDC 655620. Copies of these data can be obtained free of charge on application to CCDC, 12 Union Road, Cambridge CB2 1EZ, UK (fax: (+44) 1223-336-033; e-mail: deposit@ccdc.cam.ac.uk). Graphical plot of the final refinement cycle is shown in Figure S1

Rietveld refinement results for [CuSePh]$_\infty$ **1**: $M_r$ = 219.6, tetragonal, space group P4$_2$/$n$, $a$ = 17.131(1), $c$ = 4.1796(7)Å, $V$ = 1226.6(3)Å$^3$, $Z$ = 8, $\rho$ = 2.386 g cm$^{-3}$, parameters = 62, restraints = 40, $R_p$ = 0.0481, $R_{wp}$ = 0.0642, $R_F$ = 0.0608, $R_{WP}$(expect) = 0.0180, Goodness of fit = 3.57 for 2851 data points collected in the range of 3° <= 2θ <= 60°. $R_p = \Sigma_i|y_{i,o}-y_{i,c}|/\Sigma_i|y_{i,o}|$; $R_{wp} = [\Sigma_i w_i|y_{i,o}-y_{i,c}|^2/\Sigma_i w_i|y_{i,o}|^2]^{1/2}$; Expected $R_{wp} = R_{wp}/\chi^2$; $\chi^2 = \Sigma_i w_i|y_{i,o}-y_{i,c}|^2/(N_{obs}-N_{var})$ in which $y_{i,o}$ and $y_{i,c}$ are the observed and calculated intensities at point i of the profile, respectively. $N_{obs}$ is the number of theoretical Bragg peaks in the 2θ range. $N_{var}$ is number of the refined parameters. Statistical weights $w_i$ are normally taken as $1/y_{i,o}$. $R_F = \Sigma |I_{j,o}-I_{j,c}|/\Sigma I_{j,o}$ ($I_j$ denotes the extracted intensity of the j-th Bragg reflection).

Rietveld refinement results for [CuSeMe]$_\infty$ **2**: $M_r$ = 157.5, tetragonal, space group Pbam, $a$ = 17.296(1), $b$ = 8.6862(2), $c$ = 4.1571(1)Å, $V$ = 624.72(2)Å$^3$, $Z$ = 8, $\rho$ = 3.360 g cm$^{-3}$, parameters = 58, restraints = 16, $R_p$ = 0.0493, $R_{wp}$ = 0.0711, $R_F$ = 0.0765, $R_{WP}$(expect) = 0.0350, Goodness of fit = 2.02 for 4851 data points collected in the range of 3° <= 2θ <= 100°.

**Device Fabrication and Charge Mobility Measurement**

A suspension of solid sample of [Cu(SePh)]$_\infty$ or Cu$_2$Se in methanol was ultrasonicated for more than 12 hours to disperse the solid in the solution. Later the dispersed nanorods of [Cu(SePh)]$_\infty$ or nanocrystals of Cu$_2$Se were drop cast on the top of patterned bottom contact FET device (Figure S8). The transistor output and transfer characteristics were measured with a probe station using a Keithley K4200 semiconductor parameter analyzer inside a MBraun nitrogen glove box where oxygen and moisture level were kept below 0.1 ppm. Although a non-saturating behaviour was found for these nano-rod FET

devices, a clear effect of the gate on the current was observed. Since the saturation of the drain current was not attained, the charge-carrier mobility was extracted from the linear regime using $I_{D,lin}$ vs. $V_G$ relation.[7] At the linear regime where $V_{ds} << V_{gs}$,

$$\mu = \frac{\partial I_{ds}/\partial V_{gs}\, L}{W C_{ox} V_d}$$

(where $W$ is the channel width; $L$ is the channel length; $C_{ox}$ is the capacitance of the $SiO_2$ insulating layer; $V_{gs}$ is the gate voltage and $V_d$ is the threshold voltage).

**Inductively coupled plasma mass spectrometry.** The quadrupole-based ICP-MS spectrometer (Agilent 7500a ICP-MS, Agilent Technologies, CA, USA) was operated in time-resolved analysis (TRA) mode. The minimum integration time of 10 μs was used throughout unless specified otherwise. All isotopes were monitored in each experiment and the duration of each scan was 24 s. The acquired temporal profiles were converted into ASCII format using the ''tabchart'' function of the Chemstation software of the ICP-MS for further data processing using custom software or third party software such as Origin. A Babington nebulizer and a cooled Scott-type double-pass spray chamber were used for aerosol generation and filtration. A syringe pump (NE-1000 Single Syringe Pump, New Era Pump Systems, New York, USA) was used to maintain the sample uptake rate of 0.5 mL min$^{-1}$. Before each experiment, the ICP-MS was tuned using an aqueous multi-element standard solution (10 ng mL$^{-1}$ each of Li, Y, Co, Ce and Tl) for consistent sensitivity ($^7$Li, $^{89}$Y and $^{205}$Tl) and minimum doubly charged and oxide species levels ($^{140}$Ce).
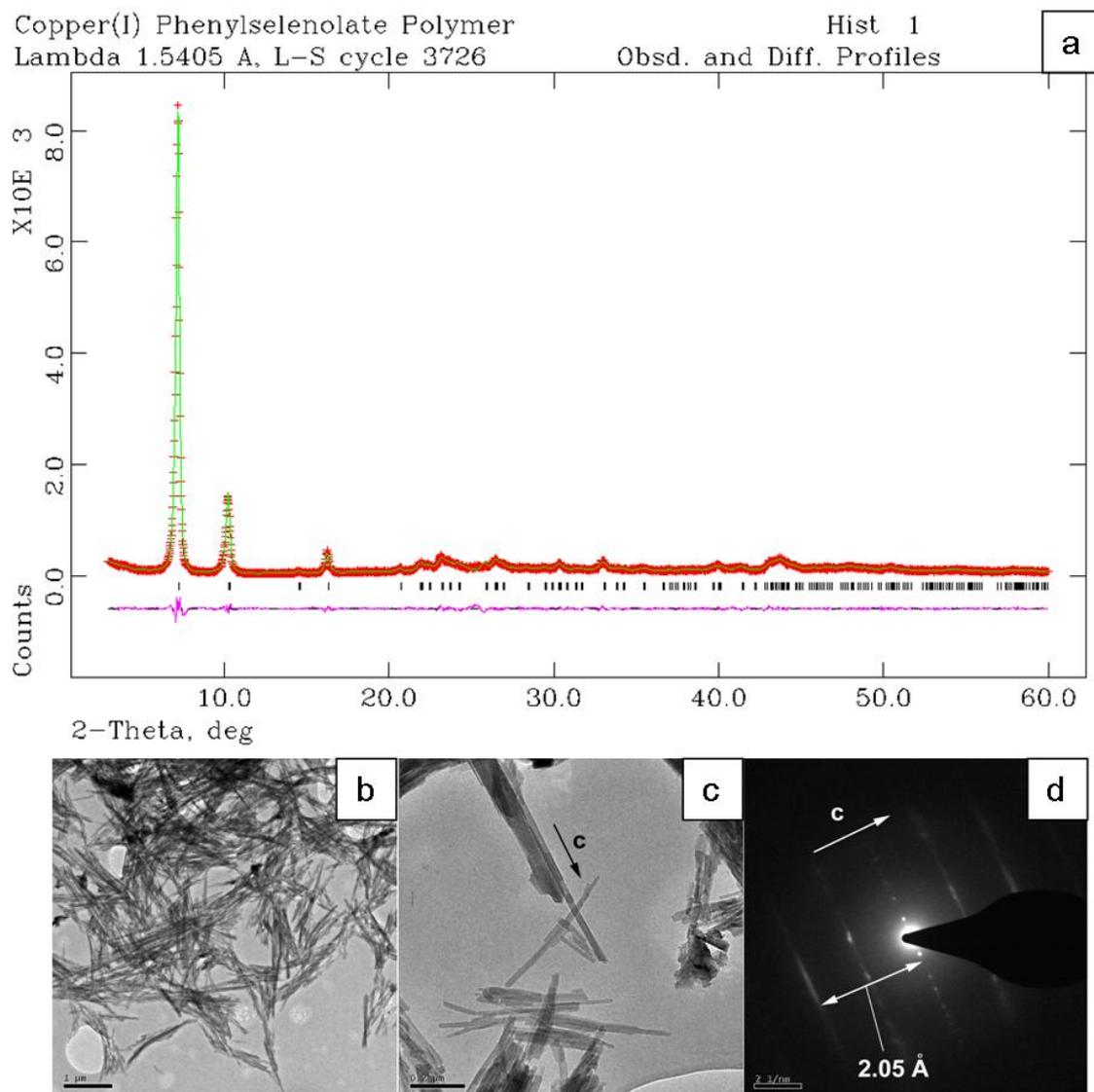
*Figure S1.*    (a) Observed (red +), calculated (green -), and difference (magenta line) profiles for final cycle of Rietveld refinement of **1**. Tick marks indicate peak positions of calculated Bragg reflections. TEM images of **1** showing nanometer size rods with magnification of 2550 (left) and 9900 (middle) respectively. The dimensions of **1** rods are $34.7 \pm 15.1$ nm in width and $624 \pm 451$ nm in length. The SAED (selected area electron diffraction) pattern of an individual nano-rod reveals that the orientation of the crystallographic *c*-axis (4.1 Å) of the **1** polymer is parallel to the long axis of the rod (right).
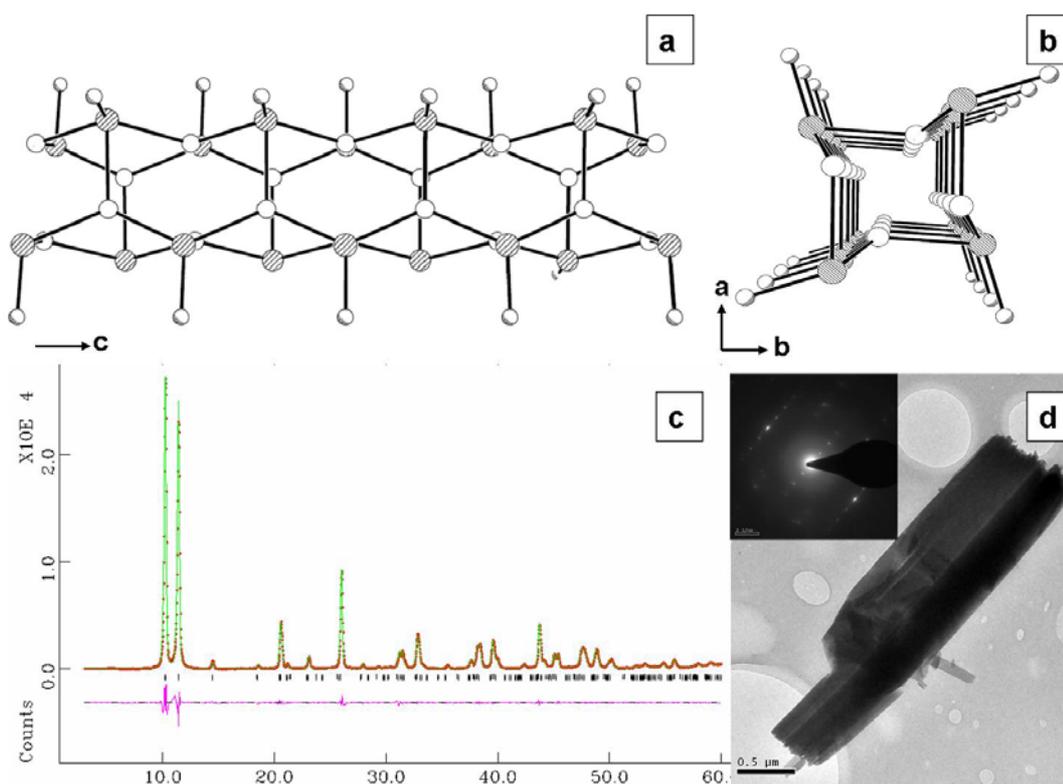
*Figure S2*. a) Perspective drawings of 1-D structure of [Cu(SeMe)]$_\infty$ **2** running along the [001] direction and b) viewed from the [001] direction. c) Observed (red +), calculated (green -), and difference (magenta line) profiles for final cycle of Rietveld refinement of **2**. Tick marks indicate peak positions of calculated Bragg reflections. d) TEM images of **2** showing nanometer size rods bundles. The dimensions of **2** rods are 73.8 ± 28.2 nm in width and 2013 ± 1128 nm in length and the corresponding SAED pattern is inserted.
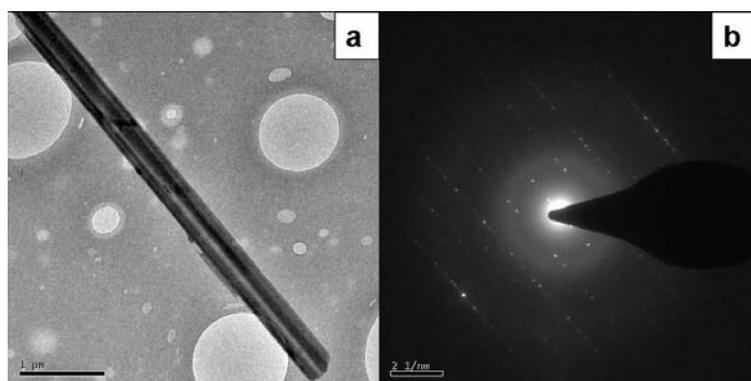


*Figure S3.* The dimensions of **3** rods are 157 ± 49 nm in width and 5733 ± 2420 μm in length (a) and the corresponding SAED (b).
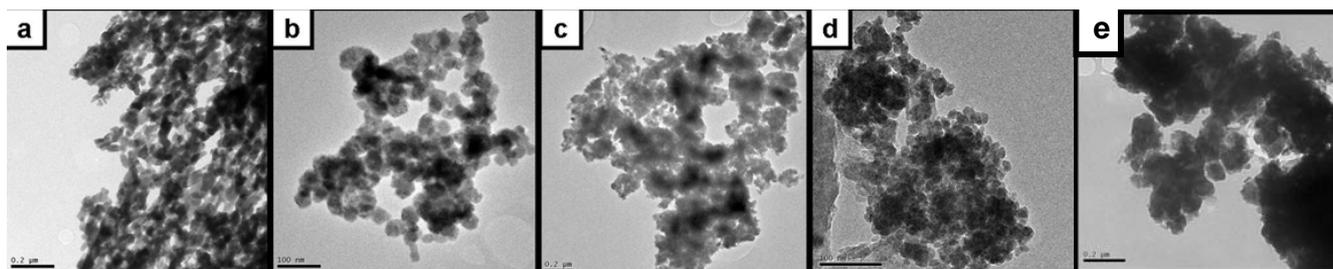
*Figure S4.* TEM images of as-formed $Cu_2Se$ nanocrystals from thermolysis of $[Cu(SePh)]\infty$ **1** under different atmosphere: (a) vacuum; (b) $N_2$; (c) Ar; and (d) air at 180 °C for 2 hr and (e) Ar at 350 °C.
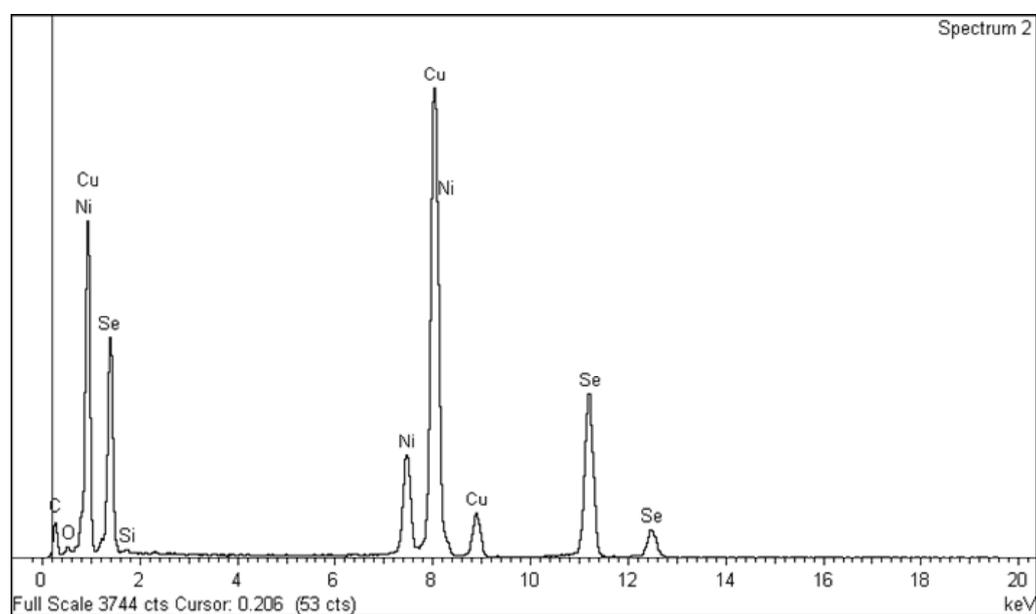


| Element | Peak Area | Area Sigma | k factor | Abs Corrn. | Weight% | Weight% Sigma | Atomic% |
|---------|-----------|------------|----------|------------|---------|---------------|---------|
| Cu K    | 56590     | 406        | 1.097    | 1.000      | 62.61   | 0.32          | 67.54   |
| Se K    | 24363     | 275        | 1.521    | 1.000      | 37.39   | 0.31          | 32.46   |
| Totals  |           |            |          |            | 100.00  |               |         |

*Figure S5*. EDS spectrum of $Cu_2Se$ obtained from the thermolysis of **1** at 180 °C under vacuum.

| Element | Peak Area | Area Sigma | k factor | Abs Corrn. | Weight % | Weight% Sigma | Atomic % |
|---------|-----------|------------|----------|------------|----------|---------------|----------|
| Cu K | 18102 | 241 | 1.366 | 0.947 | 58.01 | 0.55 | 63.19 |
| Se K | 9443 | 173 | 1.894 | 0.948 | 41.99 | 0.55 | 36.81 |
| Totals | | | | | 100.00 | | |
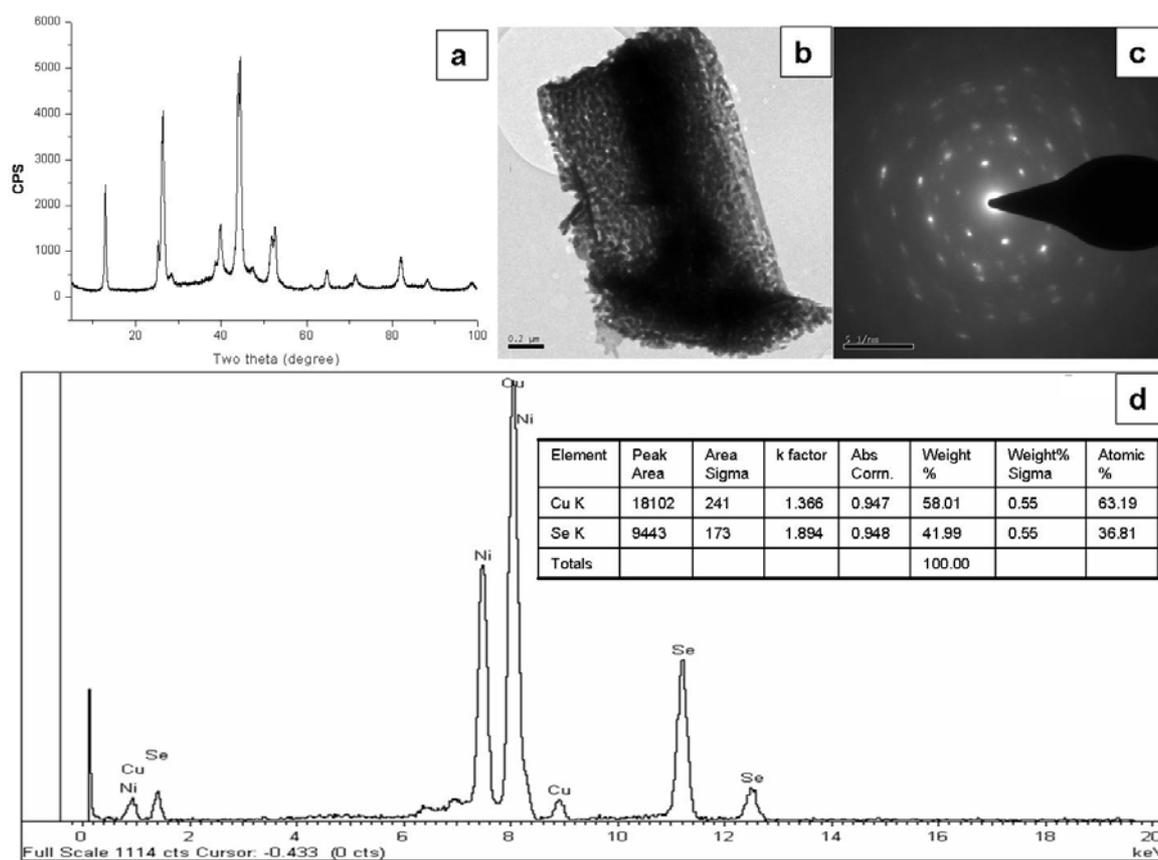
*Figure S6*. XRD pattern (a), TEM image (b), SAED (c) and EDS spectrum with a analysis table (d) of Cu$_2$Se obtained from the thermolysis of **2** at 180 $^o$C under vacuum.

| Element | Peak Area | Area Sigma | k factor | Abs Corrn. | Weight % | Weight% Sigma | Atomic % |
|---------|-----------|------------|----------|------------|----------|---------------|----------|
| Cu K | 44048 | 355 | 1.366 | 0.948 | 62.20 | 0.35 | 67.15 |
| Se K | 19289 | 242 | 1.894 | 0.949 | 37.80 | 0.35 | 32.85 |
| Totals | | | | | 100.00 | | |
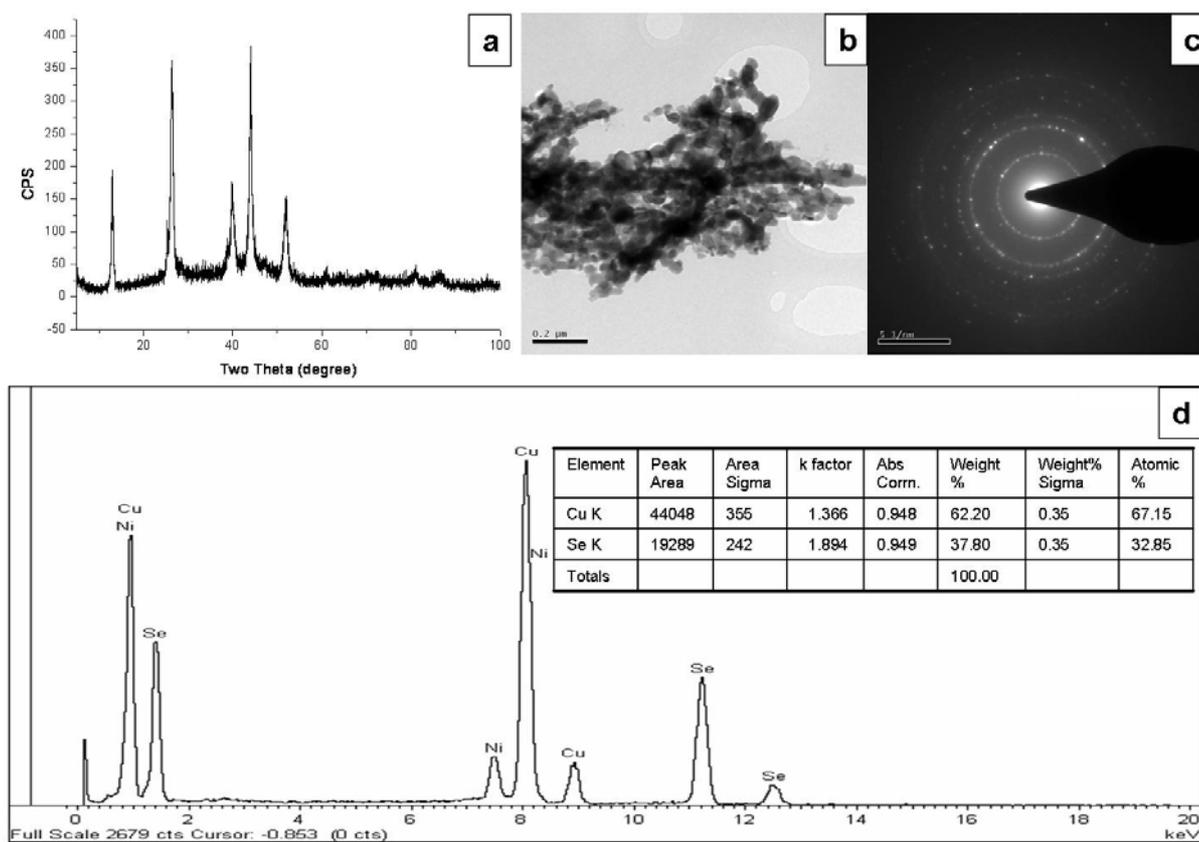
*Figure S7*. XRD pattern (a), TEM image (b), SAED (c) and EDS spectrum with a analysis table (d) of $Cu_2Se$ obtained from

the thermolysis of **3** at 180 $^o$C under vacuum.
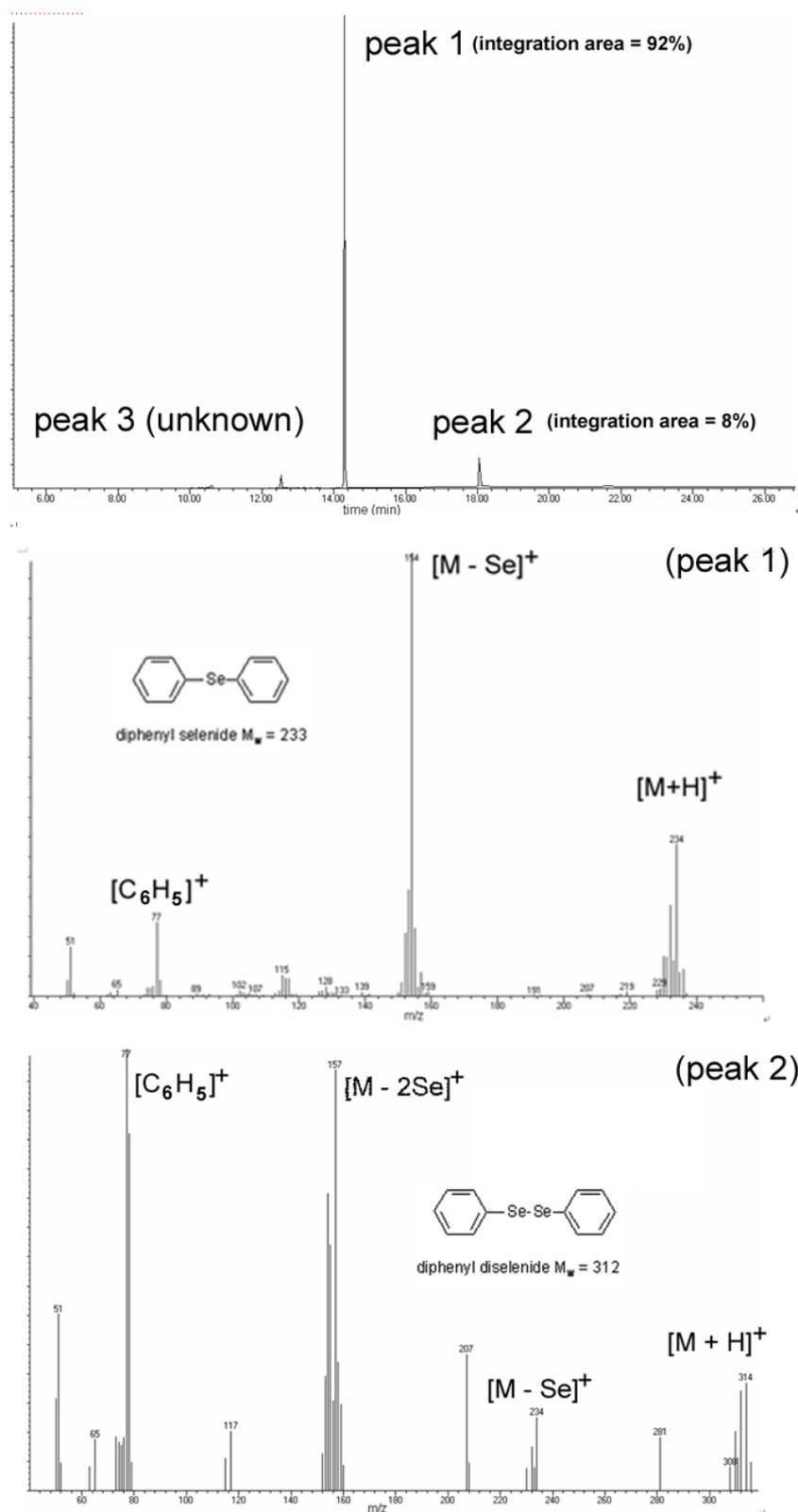
*Figure S8*.     GC-MS data of the pale yellow organic vapor dissolved in CDCl₃. There are two peaks eluted from the solution (top) and the corresponding MS spectra of these two peaks (middle and bottom).
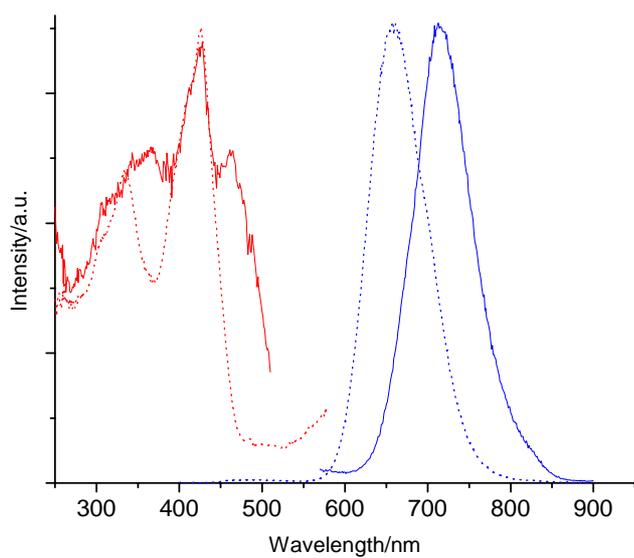
***Figure S9***.     Excitation (red) and emission (blue) spectra of the solid samples of $[Cu(SePh)]_\infty$ (—) and $[Cu(SPh)]_\infty$ (----) at

77 K.
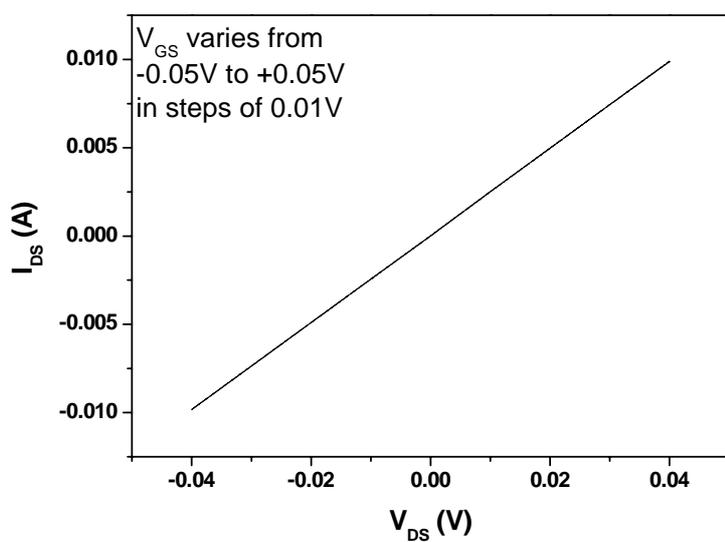


***Figure S10.***     Output characteristics of the FET device with cubic nanocrystals of $Cu_2Se$ as an active layer material.
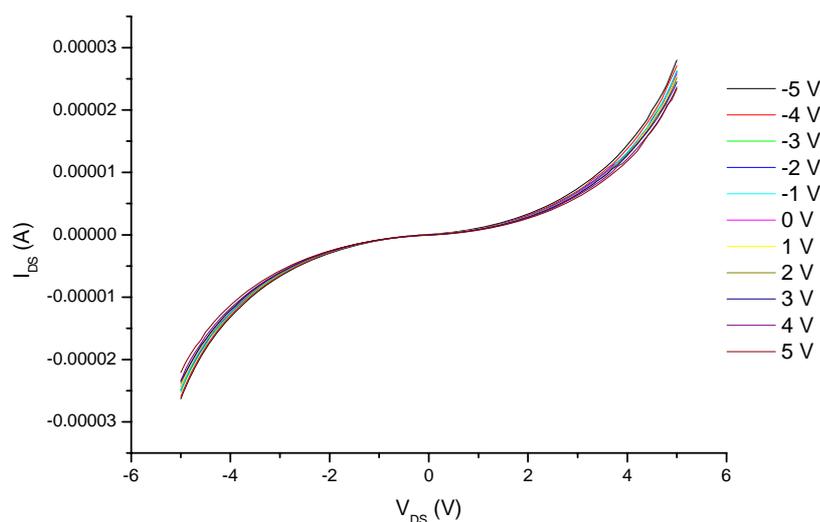
**Figure S11.** Output characteristics of the FET device with orthorhombic nanocrystals of $Cu_2Se$ as an active layer material. 10μm, 3000μm channel length and width respectively.

**References:**

[1] A. Boultif, D. Löuer. *J. Appl. Crystallogr.* **2004**, *37*, 724-731.

[2] P. -E. Werner, L. Eriksson, M. J. Westdahl. *J. Appl. Crystallogr.* **1985**, *18*, 367-370.

[3] G. S. Pawley, *J. Appl. Crystallogr.* **1981**, *14*, 357-361.

[4] W. I. F. David, K. Shankland. *DASH, Program for Structure Solution from Powder Diffraction Data*, Cambridge Crystallographic Data Center, Cambridge **2001**, (License agreement No: D/1023/2002).

[5] (a) A. C. Larson, R. B. Von Dreele, *"General Structure Analysis System (GSAS)", Los Alamos National Laboratory Report LAUR 86-748* **2004**. (b) B. H. Toby, *EXPGUI, A Graphical User Interface for GSAS, J. Appl. Crystallogr.* **2001**, *34*, 210-221.

[6] (a) P. Thompson, D. E. Cox, J. B. Hastings, *J. Appl. Crystallogr*. **1987**, *20*, 79−83. (b) L. W. Finger, D. E. Cox, A. P. Jephcoat, *J. Appl. Crystallogr*. **1994**, *27*, 892−900.

[7] S. M. Sze, *Physics of Semiconductor Devices,* second edition, Wiley, New York, **1981**, 431-496.